

Supplementary Information

Surface-decorated Nanoliposomal Leonurine Targets Activated Fibroblast-like Synoviocytes for Efficient Rheumatoid Arthritis Therapy

Shiyu Meng^{a#}, *Zhiling Song*^{a#}, *Zhuang Tang*^a, *Xiaoxue Yang*^a, *Xiao Yi*^a, *Hui Guo*^b,
Kaixiang Zhou^c, *Meirong Du*^{a,d}, *Yi Zhun Zhu*^{a*}, *Xiaolin Wang*^a

^a School of Pharmacy and State Key Laboratory of Quality Research in Chinese Medicine, Macau University of Science and Technology, Macao 999078, China

^b School of Chemical Engineering and Technology, Sun Yat-sen University, Zhuhai 519082, China

^c NHC Key Lab of Reproduction Regulation (Shanghai Institute of Planned Parenthood Research), Shanghai Key Laboratory of Female Reproductive Endocrine Related Diseases, Hospital of Obstetrics and Gynecology, Fudan University Shanghai Medical College, Shanghai 200032, China

* Corresponding authors: yzzhu@must.edu.mo (Y. Zhu), xilwang@must.edu.mo (X. Wang)

These authors contributed equally to this work.

Supporting Experimental Methods

Similarity factor (f_2) analysis

Comparison between the drug release profiles of different formulations was performed by the **similarity factor (f_2)**,

$$f_2 = 50 \log \left\{ \left(1 + \frac{1}{n} \sum_{t=1}^n (R_t - T_t)^2 \right)^{-0.5} \times 100 \right\} \#$$

where n is the sampling number, T_t and R_t are the percentage of release for the test and reference group at each time point t . f_2 factor is 100 when the test and reference profiles are identical, and approaches 0 as the dissimilarity increases.

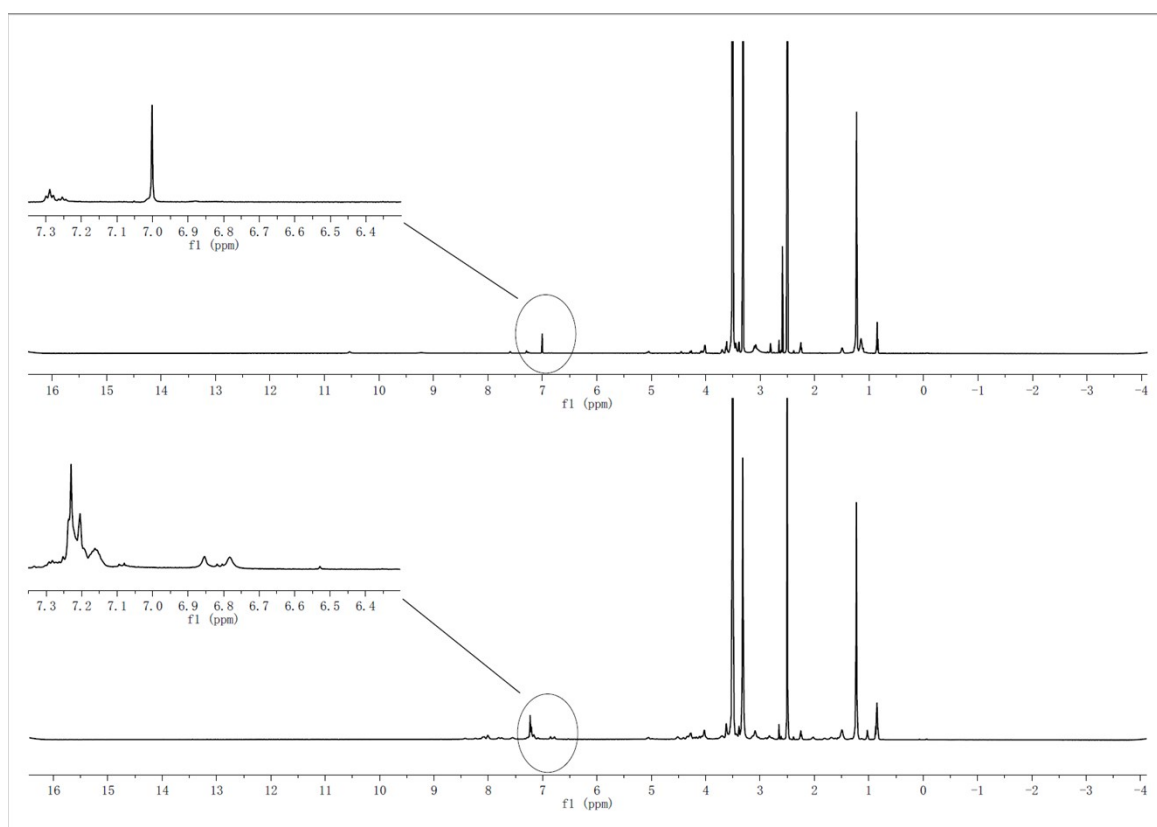


Fig. S1. ^1H NMR spectrum of (a) DSPE-PEG₅₀₀₀-MAL and (b) DSPE-PEG₅₀₀₀-HAP.

Table S1 Effect of pressure and cycle times on the particle size and PDI of nanoliposomes (n = 3)

Pressure (bar)	Cycle times	Particle size (nm)	PDI
500	1	388.7 ± 8.8	0.251 ± 0.023
	2	315.4 ± 10.0	0.200 ± 0.083
	3	223.0 ± 6.3	0.137 ± 0.020
	4	189.4 ± 4.5	0.120 ± 0.017
	5	174.5 ± 5.9	0.167 ± 0.042
	6	158.4 ± 3.1	0.148 ± 0.013
	7	153.9 ± 6.9	0.124 ± 0.029
	8	142.0 ± 2.5	0.108 ± 0.027
1000	1	101.8 ± 2.3	0.035 ± 0.029
	2	97.7 ± 3.6	0.077 ± 0.040
	3	94.4 ± 3.2	0.096 ± 0.034
	4	93.9 ± 2.2	0.104 ± 0.095
	5	93.6 ± 2.9	0.079 ± 0.012
	6	92.7 ± 3.4	0.102 ± 0.007
	7	91.2 ± 2.1	0.114 ± 0.012
	8	90.2 ± 2.9	0.115 ± 0.032
1500	1	98.8 ± 1.4	0.032 ± 0.005
	2	95.4 ± 2.3	0.105 ± 0.048
	3	93.6 ± 2.0	0.116 ± 0.015
	4	91.0 ± 3.7	0.157 ± 0.029
	5	87.6 ± 2.8	0.149 ± 0.017
	6	86.7 ± 1.6	0.173 ± 0.044
	7	84.3 ± 2.5	0.122 ± 0.030
	8	84.2 ± 2.1	0.138 ± 0.041

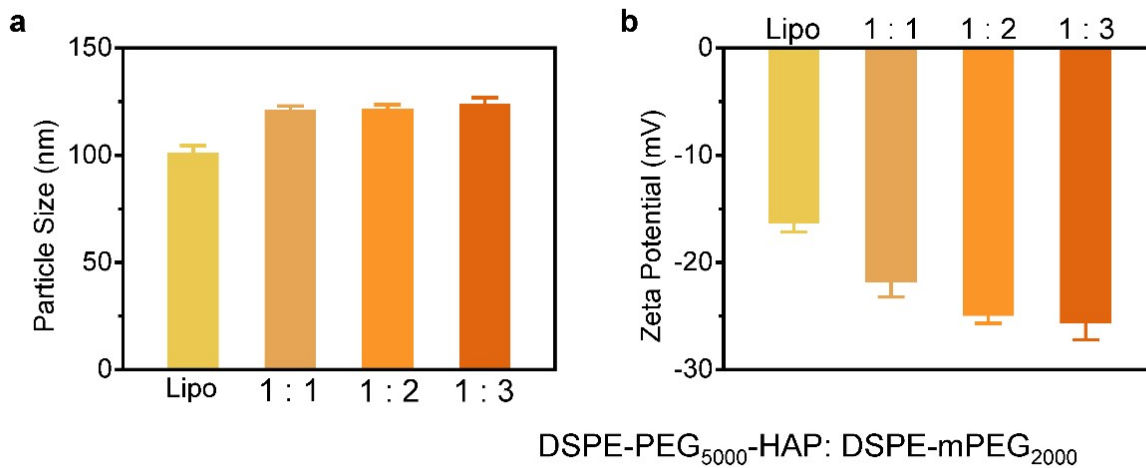


Fig. S2. Particle size (a) and zeta potential (b) of Lipo@Leo with different DSPE-PEG₅₀₀₀-HAP: DSPE-MPEG₂₀₀₀ weight ratios. Data are presented as mean \pm SD (n = 3).

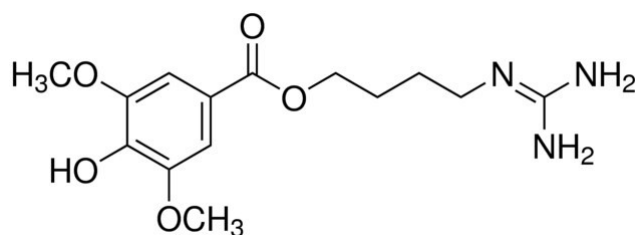


Fig. S3. The structural formula of Leonurine.

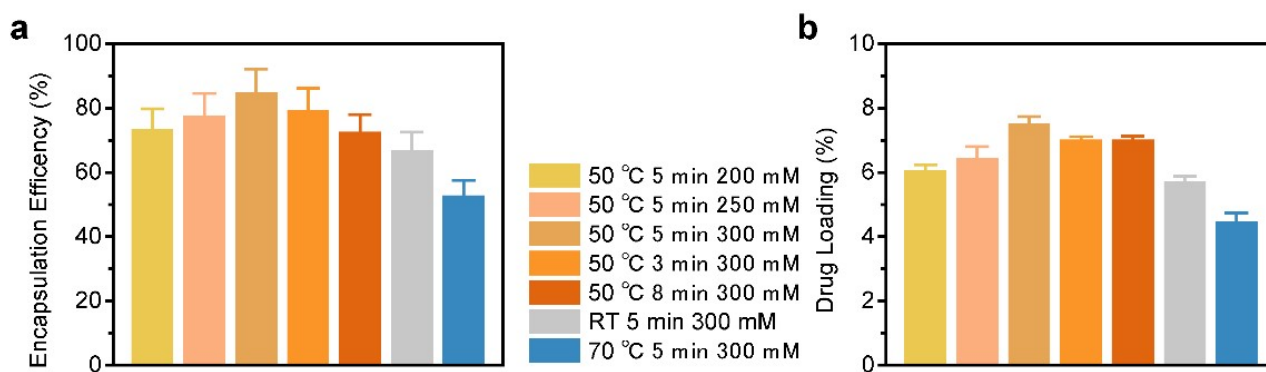


Fig. S4. Impact of ammonium sulfate concentration, temperature, and drug incubation time on the encapsulation efficiency (a) and drug loading (b) of HAP-Lipo@Leo. Data are presented as mean \pm SD (n = 3).

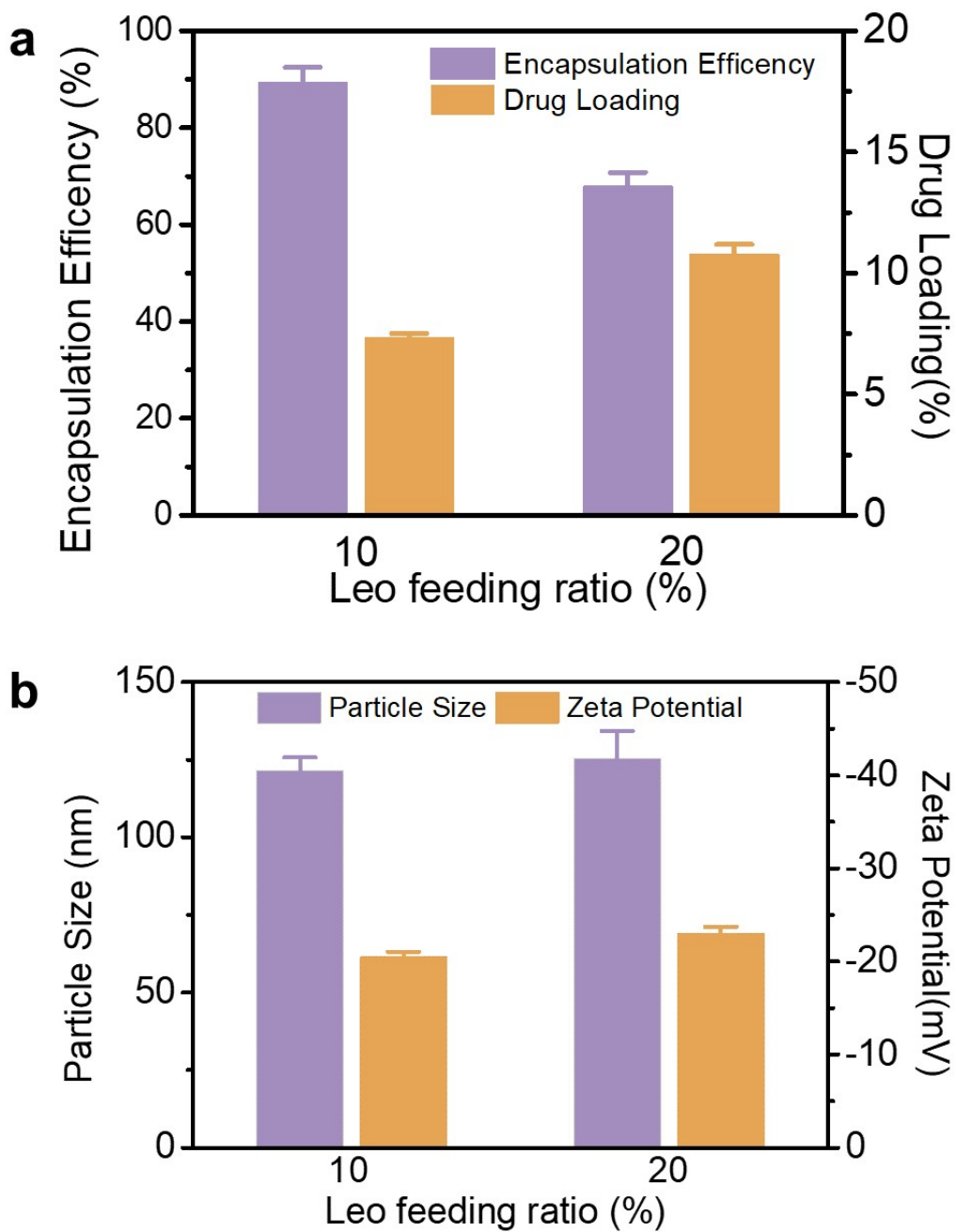


Fig. S5. Synthesis and characterization of HAP-Lipo@Leo with different Leo/total lipid feed ratios. (a) Encapsulation efficiency and drug loading; (b) Particle size and zeta potential. Data are presented as mean \pm SD (n = 3).

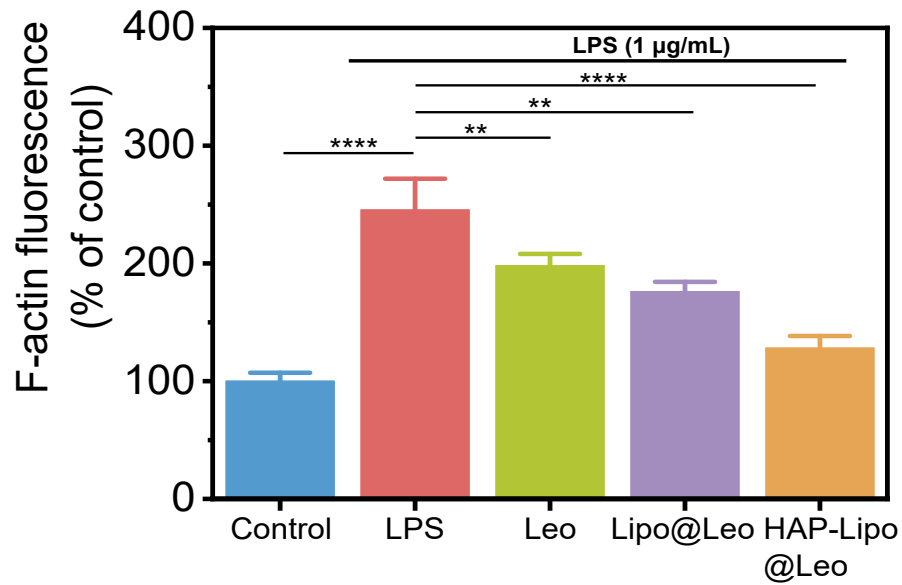


Fig. S6. Fluorescence intensity of phalloidin-stained F-actin after different treatments. Variance among groups at day 30 was determined by one-way ANOVA with Tukey post-hoc test (* $P < 0.05$, ** $P < 0.01$, *** $P < 0.001$, **** $P < 0.0001$).

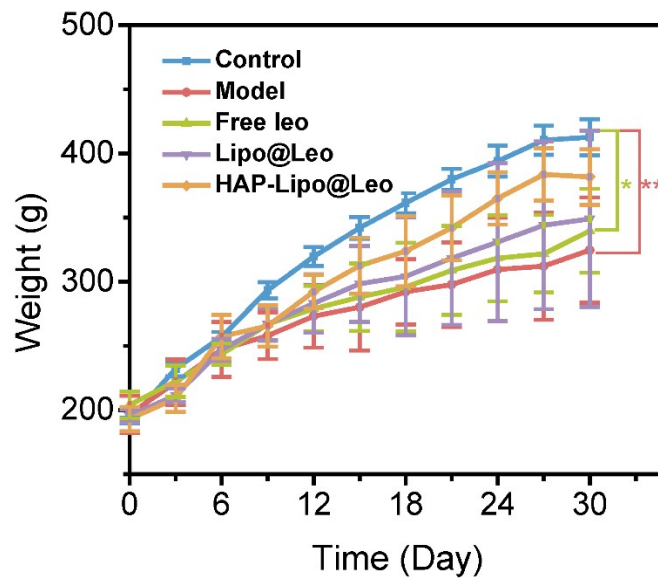


Fig. S7. Body weight of healthy rats and AIA rats after treatment with PBS, Free Leo, Lipo@Leo, and HAP-Lipo@Leo. Data are presented as mean \pm SD ($n = 6$). Variance among groups at day 30 was determined by one-way ANOVA with Tukey post-hoc test (* $P < 0.05$, ** $P < 0.01$, *** $P < 0.001$, **** $P < 0.0001$).

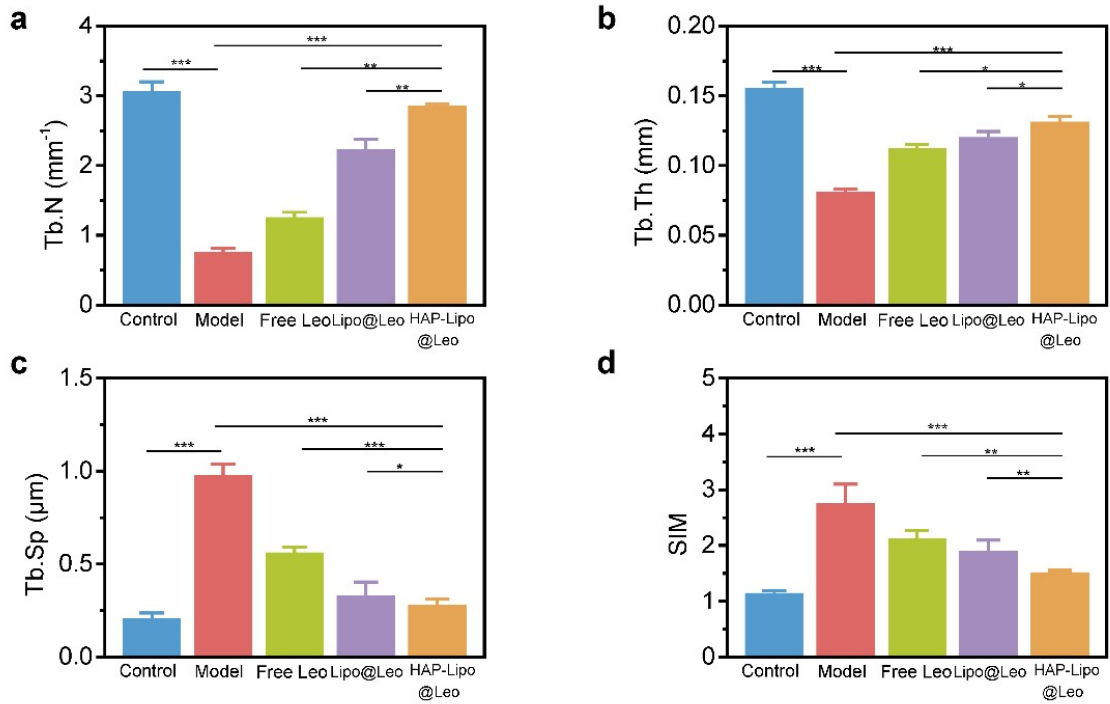


Fig. S8. Histomorphometry parameters obtained from analyses of the micro-CT data. (a) Tb.N: Trabecular number, (b) Tb.Th: Trabecular thickness; (c) Tb.Sp: Trabecular bone spacing, (d) SMI: Structure model index. Data are shown as the mean \pm SD ($n = 6$); Variance among groups was determined by one-way ANOVA with Tukey post-hoc test (* $p < 0.05$, ** $p < 0.01$, *** $p < 0.001$ and **** $p < 0.0001$).

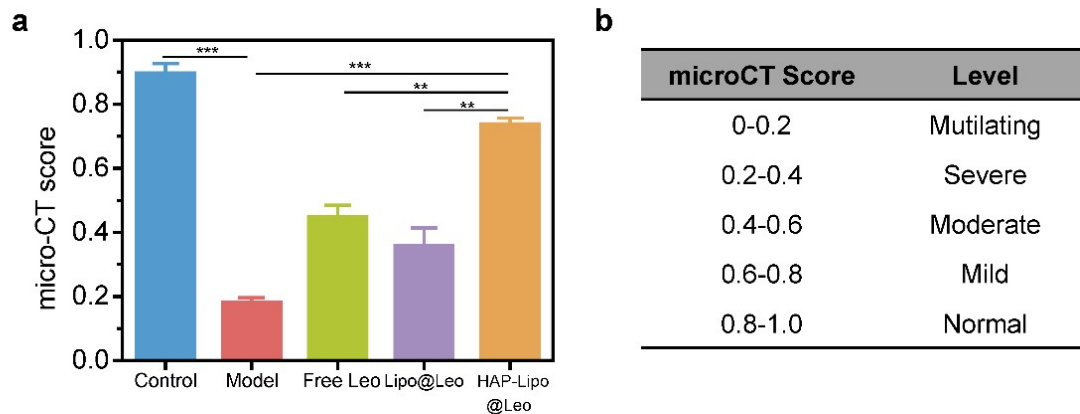


Fig. S9. Micro-CT score of the hind paws of normal rats and AIA rats with different treatments. The micro-CT score was obtained according to five disease-related micro-CT analysis indexes: BMD, BV/TV, TMD, Tb.N and total porosity. Data are shown as the mean \pm SD ($n = 6$); Variance among groups was determined by one-way ANOVA with Tukey post-hoc test (* $p < 0.05$, ** $p < 0.01$ and *** $p < 0.001$).

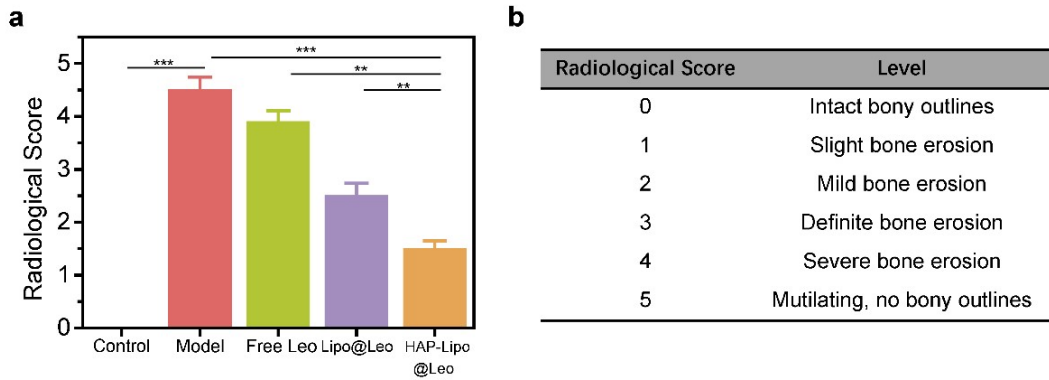


Fig. S10. The radiological score of AIA rats. The Radiological score was obtained according to micro-CT images. Data are shown as the mean \pm SD (n = 6); Variance among groups was determined by one-way ANOVA with Tukey post-hoc test (*p < 0.05, **p < 0.01, and ***p < 0.001).

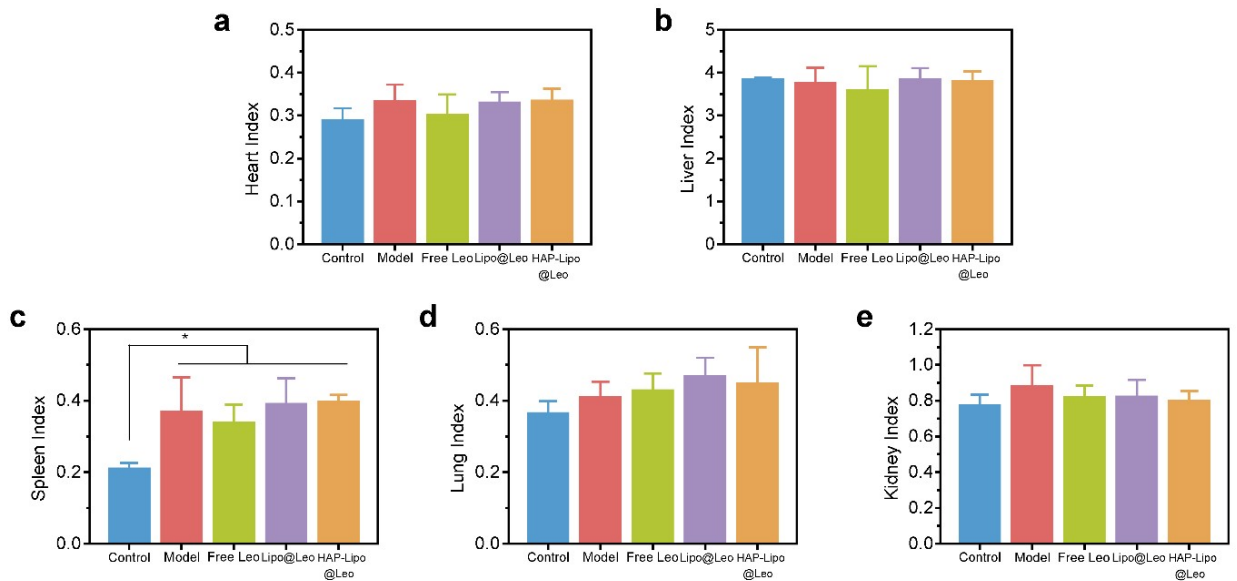


Fig.S11. The effect of different treatments on major organ index of rats. (a) Heart index. (b) Liver index. (c) Spleen index. (d) Lung index. (e) Kidney index. The data are expressed as mean \pm SD (n = 6). Variance among groups was determined by one-way ANOVA with Tukey post-hoc test (*P < 0.05, ** P < 0.01, *** P < 0.001, ****P < 0.0001).